CHINESE OPTICS LETTERS

Vol. 22, No. 4 | April 2024

High-power all-fiber linearly polarized Yb-doped chirped pulse amplifier based on active polarization control

Tao Wang (王 涛)[1,†], Shuai Ren (任 帅)[1,2,†], Hongxiang Chang (常洪祥)[1,†], Bo Ren (任 博)[1], Kun Guo (郭 琨)[1], Can Li (李 灿)[1*], Pengfei Ma (马鹏飞)[1,3,4], Jinyong Leng (冷进勇)[1,3,4], and Pu Zhou (周 朴)[1**]

[1] College of Advanced Interdisciplinary Studies, National University of Defense Technology, Changsha 410073, China

[2] School of Information and Communications, National University of Defense Technology, Wuhan 430035, China

[3] Nanhu Laser Laboratory, National University of Defense Technology, Changsha 410073, China

[4] Hunan Provincial Key Laboratory of High Energy Laser Technology, National University of Defense Technology, Changsha 410073, China

[†]These authors contributed equally to this work.

*Corresponding author: lc0616@163.com

**Corresponding author: zhoupu203@163.com

Received August 29, 2023 | Accepted December 11, 2023 | Posted Online April 17, 2024

High-power ultrafast laser amplification based on a non-polarization maintaining fiber chirped pulse amplifier is demonstrated. The active polarization control technology based on the root-mean-square propagation (RMS-prop) algorithm is employed to guarantee a linearly polarized output from the system. A maximum output power of 402.3 W at a repetition rate of 80 MHz is realized with a polarization extinction ratio (PER) of $>$ 11.4 dB. In addition, the reliable operation of the system is verified by examining the stability and noise properties of the amplified laser. The M^2 factor of the laser beam at the highest output power is measured to be less than 1.15, indicating a diffraction-limited beam quality. Finally, the amplified laser pulse is temporally compressed to 755 fs with a highest average power of 273.8 W. This is the first time, to the best of our knowledge, that the active polarization control technology was introduced into the high-power ultrafast fiber amplifier.

Keywords: active polarization control; root-mean-square propagation algorithm; linearly polarized laser; chirped pulse amplification; femtosecond laser; fiber laser.

DOI: 10.3788/COL202422.041403

1. Introduction

High-power ultrafast fiber lasers with high beam quality have been widely applied in the industrial sector and the frontier science field[1–4]. In the context of the power scaling of ultrafast fiber lasers, it is imperative to mitigate the nonlinear effects, including stimulated Raman scattering (SRS) and nonlinear phase accumulation, as well as the transverse mode instability (TMI) effect[5–7]. Up to date, the average power of ultrafast fiber lasers has approached more than 1 kW based on the free-space coupled structure[8]; whereas for the all-fiber configuration, the highest power of the ultrafast laser operating in the single pulse mode is 440.6 W at a repetition rate of 80 MHz[9]. For a repetition rate up to GHz, it makes the high-power amplification more reliable and the pulse sequence manipulation more flexible, e.g., burst mode operation, particularly in an all-fiber configuration. So far the highest power has been demonstrated to be 108 W[10]. It should be noted that the well-known chirped pulse amplification (CPA) system that is routinely employed for power scaling of ultrafast fiber lasers generally operates in the linearly polarized regime[11–13], due to the polarization dependent characteristic of the corresponding pulse compressor. Moreover, linearly polarized lasers are also strongly required in many applications, such as fiber laser coherent beam combining (CBC)[14–16] and nonlinear frequency conversion[17,18].

Generally, a polarization-maintaining (PM) fiber system is mandatory for the laser generation with linear polarization[6,19,20], including linearly polarized seed lasers and all-PM fiber amplifiers, of which the costs are more expensive than the non-PM counterparts. In addition, the fabrication and handling technologies of PM fibers are also more complicated and challenging than that of non-PM fibers. More importantly, it has been verified that there exist correlations between the laser polarization state and both the nonlinear effects and the TMI. Specifically, the Raman and Brillouin gain coefficients in the PM fibers are higher than those in the non-PM fibers[21-23]. Additionally, researchers have demonstrated that PM fiber amplifiers exhibit significantly lower TMI thresholds than non-PM versions[24-27]. As such, a non-PM fiber amplifier is more preferable for alleviating the limitations on the power

scaling of different types of lasers. For instance, the highest output powers delivered from a PM fiber amplifier in the broadband spectrum and narrow linewidth laser were, respectively, 3 kW[28] and 5 kW[29,30], which are notably lower than that of the non-PM fiber amplifiers[31,32].

To realize a linearly polarized high-power output from a non-PM fiber amplifier, a feasible scheme is the utilization of polarization control technique[33,34], which was originally developed in the optical fiber communication[35] and fiber sensing systems[36], for mitigating the polarization mode dispersion. Over the last decade, significant advancements have been made in the polarization control of high-power fiber amplifiers. In 2010, Goodno *et al.* reported the successful implementation of an active polarization control to a non-PM fiber amplifier with an output power exceeding 1 kW, which was then applied to fiber laser CBC systems[37,38]. In 2017, linearly polarized narrow linewidth lasers with an average power of, respectively, 1 kW[39] and 1.43 kW[40] were realized from non-PM fiber amplifiers with the active polarization control technique based on the stochastic parallel gradient descent (SPGD) algorithm. After that, IPG Photonics Corp. presented a 2.5 kW linearly polarized laser output by controlling the polarization state of the input signal of a non-PM fiber amplifier, while more details of the control algorithm have not been disclosed[41]. More recently, Ren *et al.* demonstrated a narrow linewidth non-PM all-fiber amplifier that delivers 3.38 kW laser output with a PER of 12.2 dB, with the aid of active polarization control based on the root-mean-square propagation (RMS-prop) algorithm[42]. It is noted that previous demonstrations concerning active polarization control of non-PM fiber amplifiers were mostly focused on narrow linewidth lasers, while its effectiveness on the power scaling of ultrafast laser is yet to be verified.

In this paper, the feasibility of utilizing the active polarization control technology to achieve high-power linearly polarized ultrafast laser from a non-PM fiber amplifier was experimentally investigated. The RMS-prop algorithm was employed to demonstrate the adaptive control. Ultimately, a linearly polarized output with a highest average power of 402.3 W at a repetition rate of 80 MHz and a PER of 11.4 dB was realized. Further power scaling was limited by the SRS effect and the polarization degradation under strong nonlinear effects. This is the first time, to the best of our knowledge, that active polarization control technology has been introduced into high-power ultrafast fiber amplifiers. The laser pulse was compressed to 755 fs by a pair of diffraction gratings. It is believed that the active polarization control technique is a promising way to realize high-power linearly polarized ultrafast lasers from non-PM fiber amplifiers.

2. Experimental Setup

The experimental setup of the high-power CPA system based on the active polarization control is presented in Fig. 1. The seed source was an all-PM mode-locked fiber laser, of which the output has a pulse duration of 6 ps and a repetition rate of 80 MHz, as reported in our previous work[9]. The seed laser was stretched by two cascaded chirped fiber Bragg gratings (CFBGs) with a minimum 3-dB bandwidth of 11 nm to a full width of 2 ns, to reduce the peak power and mitigate the nonlinear effects during pulse amplification. After stretching, the linearly polarized laser pulse was injected into a polarization controller (PC), which is composed of four piezoelectric ceramics[40,42]. The polarization state of the laser signal can be electronically adjusted by manipulating the analog voltage signal that is applied to each piezoelectric ceramic, which has a 3-dB bandwidth of 16 kHz. Subsequently, the laser signal was successively amplified by three non-PM all-fiber amplifiers. The pre-amplifier 1 (PA1) was constructed with a piece of 1-m single-mode Yb-doped fiber (YDF) with a core/cladding diameter of 6/125 μm and was pumped by a 976-nm single-mode laser diode (LD); whereas the pre-amplifier 2 (PA2) employed a piece of 1.3 m double-cladding YDF with a core/cladding diameter of 10/125 μm, and was cladding-pumped by a 976 nm multi-mode LD. After being boosted to an average power of 9 W, the laser pulse was passed through a filter to remove the amplified spontaneous emission (ASE) that was produced by the PAs and a circulator (Cir) to protect the front system. The main amplifier was constructed with a piece of 5.2-m YDF with a core/cladding diameter of 25/400 μm, a cladding absorption coefficient of 1.7 dB/m, and a core numerical aperture (NA) of 0.06, which was pumped by 976-nm multi-mode laser diodes (LDs) via a $(6+1)\times 1$ pump/signal combiner. The main amplifier was

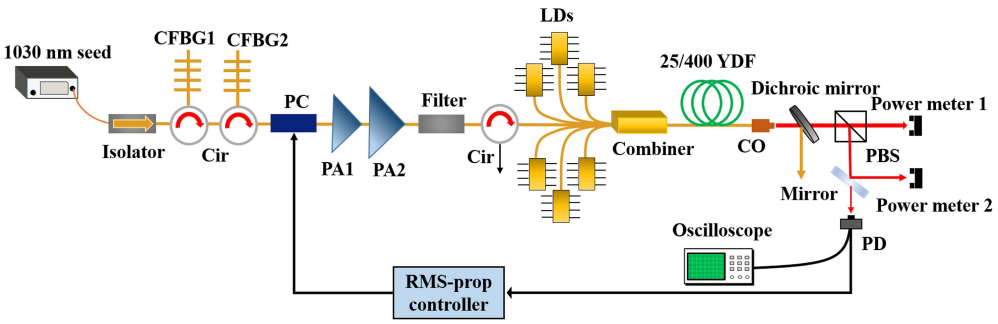

Fig. 1. Experimental setup of the high-power CPA system based on the active polarization control technology. Cir, circulator; CFBG, chirped fiber Bragg grating; PC, polarization controller; PA, pre-amplifier; LD, laser diode; YDF, Yb-doped fiber; CO, collimator; PBS, polarization beam splitter; PD, photodetector.

placed on a water-cooled plate, and the amplified laser was delivered to the free space through a fiber collimator (CO).

The output laser first passed through a dichroic mirror to separate the un-absorbed pump and the signal, which was then split into two beams by a polarization beam splitter (PBS). The horizontal polarized light was collected by power meter 1, while the vertical polarized light was sampled by a photodetector (PD) through a reflective mirror with a reflectivity of ~99.9% for monitoring the linearly polarized power by power meter 2. Afterward, the analog voltage signal that was generated by the PD was processed by the RMS-prop controller to produce a control signal for the PC for minimizing the power of the vertical polarized light while in the meantime maximizing that of the horizontal polarized light. The RMS-prop algorithm is an optimized neural network algorithm that exhibits high control accuracy and fast convergence[42,43], enabling effective and real-time active polarization control.

3. Results and Discussions

The output power and PER evolution of the main amplifier were first investigated in detail, and the results are shown in Figs. 2(a) and 2(b), respectively. With the enhancement of the pump power, the output power scaled linearly with a slope efficiency of 76.9%; whereas for the PER, it remained at around 12 dB when the output power was lower than 400 W. At the output power of 402.3 W, a PER of 11.4 dB was measured, corresponding to a highest horizontal linearly polarized light of 375 W, which shares 93.2% of the total output. Further increasing the operation power led to an apparent degrading of the PER to < 10 dB, mostly induced by the enhanced nonlinear effects, such as self-phase modulation and stimulated Raman scattering (SRS)[44,45], as well as thermal effects under high-power operation. By employing a PC with a higher bandwidth and improving the control accuracy of the algorithm, it is expected to obtain a higher PER from the non-PM fiber amplifier. Actually, at the output power of 402.3 W, the SRS effect has emerged at around 1080 nm, as shown in Fig. 2(c), which presents the measured spectra at selected output powers. At the highest power, the output spectrum has a 3-dB bandwidth of 3.13 nm. Moreover, the PER at the open loop state was also measured and shown in Fig. 2(b). As expected, the linear polarization property of the output was very poor even at the low power operation regime, and the corresponding PER quickly decreased to < 2.5 dB when the average power was > 400 W. Essentially, those results indicate that the adoption of the active polarization control to an ultrafast non-PM fiber amplifier can realize a desired linearly polarized output under high-power operation. In addition, the M^2 factors of the output in the x- and y-directions at different powers are depicted in Fig. 2(d), in which the corresponding beam profiles are also shown. It can be observed that the output laser remained a near diffraction-limited beam quality, and the M^2 factors of 1.14 and 1.13, respectively, in the x- and y-directions were measured at the output power of 402.3 W.

To characterize the stability of the CPA system at specifically the highest output power of 402.3 W, the temporal intensity evolution that was detected by the PD before and after polarization control was first measured, as shown in Fig. 3(a). As can be observed from the figure, the temporal signal quickly converged from a high amplitude at the open loop state to a minimum value and remained relatively stable, verifying the reliability of the active polarization control. Figure 3(b) demonstrates the radio frequency (RF) spectrum at the fundamental repetition frequency with a resolution bandwidth (RBW) of 1 kHz, and a signal-to-noise ratio (SNR) as high as 76.6 dB was estimated. The RF spectrum in a frequency range of 1 GHz with an RBW of 10 kHz is presented in the inset, in which no spurious peaks can be observed. Figure 4(a) shows the measured phase noise (PN) spectrum in a frequency range of 10 Hz–10 MHz and the corresponding integrated time jitter (TJ), which were measured by employing a commercial cross-correlation phase noise analyzer, as reported in our previous work[46,47]. In the low frequency range between 10 Hz and 2 kHz, the amplitude of the PN

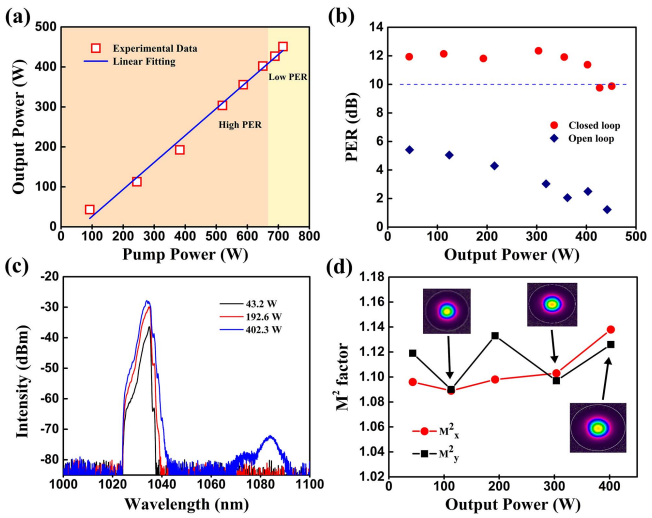

Fig. 2. Output characteristics of the main amplifier. (a) Output power versus the pump power. (b) PER evolution with and without active polarization control. (c) Output spectra. (d) M^2 factor and corresponding beam profile at different output powers.

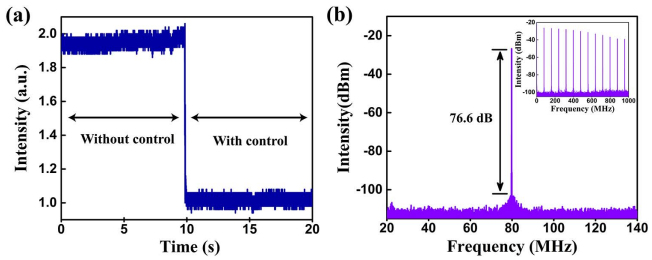

Fig. 3. Stability properties of the main amplifier at the output power of 402.3 W. (a) Temporal intensity fluctuations at the closed and open loop states. (b) RF spectrum at the fundamental repetition frequency. Inset: RF spectrum in the frequency range of 1 GHz.

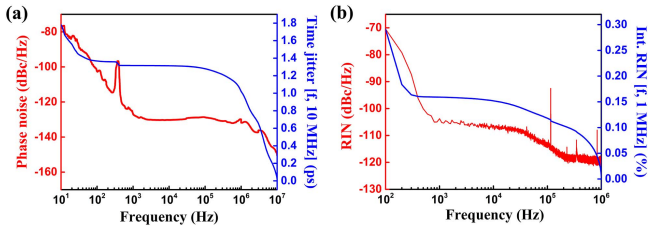

Fig. 4. Noise properties of the main amplifier at the output power of 402.3 W. (a) PN and TJ in the frequency of 10 Hz–10 MHz. (b) RIN spectrum and integrated RIN in the frequency range of 100 Hz–1 MHz.

rolled off rapidly, owing to the domination of technical noises in this frequency range, such as pump power variations and inevitable environmental disturbance, e.g., mechanical vibration and temperature fluctuation[48], which most probably caused the formation of the narrow spike located at ∼390 Hz. In the frequency range of 2 kHz–1 MHz, the PN spectrum was relatively flat with an amplitude of −131.8 dBc/Hz@1 MHz, which was then gradually decreased to −150.5 dBc/Hz@10 MHz. In addition, the TJ integrated from 10 Hz to 10 MHz was calculated to be 1.78 ps. The relative intensity noise (RIN) spectrum was measured with a low-noise photodetector, a low-pass filter with a cut-off frequency of 1.9 MHz, and an electrical spectrum analyzer, and the results are shown in Fig. 4(b). Basically, the laser RIN also presented a rapid amplitude dropped behavior in the low frequency range of 100 Hz to 2 kHz. At higher frequencies, the amplitude of the RIN spectrum decreased monotonically and approached an asymptotic level of −119 dBc/Hz@1 MHz. In addition, the integrated RIN in the examined frequency range (100 Hz–1 MHz) was calculated to be 0.29%, as shown in Fig. 4(b).

Finally, the horizontal linearly polarized laser under active polarization control was compressed by a pair of diffraction gratings, which have a central wavelength of 1030 nm with a line density and Littrow angle of 1739 lines/mm and 63.6°, respectively. The recorded autocorrelation traces of the compressed pulse at different output powers are presented in Fig. 5. It can be seen that the pulse width decreased with the increasing of the output power, mostly caused by the self-phase-modulation induced spectral broadening, as shown in Fig. 2(c). In addition, the pulse pedestal shown in the figure was mainly attributed to the uncompensated high-order dispersions and accumulated nonlinear phase shift, which was calculated to be 1.41π radians at the highest output power. Particularly, at the output power of 402.3 W, in which only the 375 W horizontal polarized component was incident to the compressor, the proportion of the pulse energy in the main peak was estimated to be 56.2%. Considering the compression efficiency of ∼73%, the compressed pulse has a highest average power of 273.8 W with a pulse energy of 3.4 μJ and a pulse width of 755 fs, assuming a Gaussian fitting to the autocorrelation trace. After excluding the pulse energy in the pedestal, the maximum peak power of the compressed pulse was calculated to be 2.55 MW.

4. Conclusion

In conclusion, high-power ultrafast laser amplification was demonstrated in an all-fiber non-PM CPA system based on active polarization control. By employing the RMS-prop algorithm, a linearly polarized laser with a maximum output power of 402.3 W and a PER of 11.4 dB was obtained. The output laser maintained excellent beam quality during the power scaling progress, and M^2 factors of 1.14 and 1.13, respectively, in the x- and y-directions at the highest power were measured. In addition, the stability and noise properties of the amplified laser were also examined, verifying the reliability of the polarization control scheme. After pulse compression by a pair of diffraction gratings, the amplified laser pulse was temporally shortened to 755 fs with a maximum average power of 273.8 W and a peak power of 2.55 MW. To the best of our knowledge, this is the first time to introduce the active polarization control technology into the high-power ultrafast fiber amplifier. Future work involves applying this technique to the ultrafast laser coherent beam combining system.

Acknowledgements

This work was supported by the Director Fund of State Key Laboratory of Pulsed Power Laser Technology (No. SKL2020ZR02) and the Postgraduate Scientific Research Innovation Project of Hunan Province (No. QL20220007).

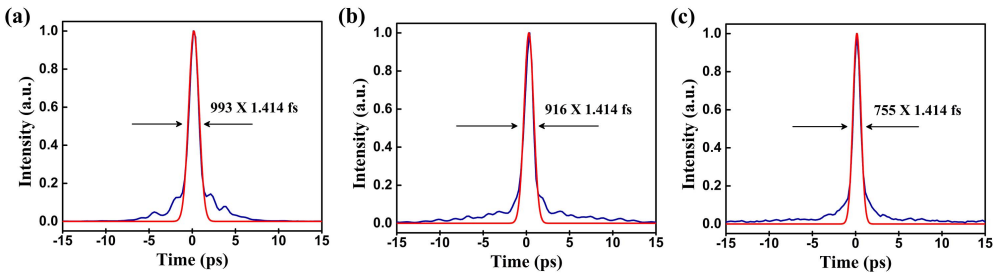

Fig. 5. Autocorrelation trace of the compressed pulse at the output power of (a) 43.2 W, (b) 192.6 W, and (c) 402.3 W. The blue and red curves, respectively, denote the measured and fitted autocorrelation traces.

References

1. M. Malinauskas, A. Žukauskas, S. Hasegawa, *et al.*, "Ultrafast laser processing of materials: from science to industry," Light Sci. Appl. **5**, e16133 (2016).
2. M. Müller, C. Aleshire, A. Klenke, *et al.*, "10.4 kW coherently combined ultrafast fiber laser," Opt. Lett. **45**, 3083 (2020).
3. R. Klas, A. Kirsche, M. Gebhardt, *et al.*, "Ultra-short-pulse high-average-power megahertz-repetition-rate coherent extreme-ultraviolet light source," PhotoniX **2**, 4 (2021).
4. J. Buldt, T. Heuermann, Z. Wang, *et al.*, "High-power two-color plasma-based THz generation driven by a Tm-doped fiber laser," Opt. Lett. **48**, 3403 (2023).
5. D. J. Richardson, J. Nilsson, and W. A. Clarkson, "High power fiber lasers: current status and future perspectives," J. Opt. Soc. Am. B **27**, B63 (2010).
6. M. N. Zervas and C. A. Codemard, "High power fiber lasers: a review," IEEE J. Sel. Top. Quantum Electron. **20**, 219 (2014).
7. J. Zuo and X. Lin, "High-power laser systems," Laser Photonics Rev. **16**, 2100741 (2022).
8. C. Gaida, M. Gebhardt, T. Heuermann, *et al.*, "Ultrafast thulium fiber laser system emitting more than 1 kW of average power," Opt. Lett. **43**, 5853 (2018).
9. T. Wang, C. Li, B. Ren, *et al.*, "High-power femtosecond laser generation from an all-fiber linearly polarized chirped pulse amplifier," High Power Laser Sci. Eng. **11**, e25 (2023).
10. Y. Liu, J. Wu, X. Wen, *et al.*, ">100 W GHz femtosecond burst mode all-fiber laser system at 1.0 μm," Opt. Express **28**, 13414 (2020).
11. D. Strickland and G. Mourou, "Compression of amplified chirped optical pulses," Opt. Commun. **55**, 447 (1985).
12. Y. Zhang, J. Wang, H. Teng, *et al.*, "Double-pass pre-chirp managed amplification with high gain and high average power," Opt. Lett. **46**, 3115 (2021).
13. V. Shumakova, V. F. Pecile, J. Fellinger, *et al.*, "Spectrally tunable high-power Yb:fiber chirped-pulse amplifier," Photonics Res. **10**, 2309 (2022).
14. A. Klenke, M. Müller, H. Stark, *et al.*, "Coherent beam combination of ultrafast fiber lasers," IEEE J. Sel. Top. Quantum Electron. **24**, 0902709 (2018).
15. S. Chen, T. Zhou, Q. Du, *et al.*, "Broadband spectral combining of three pulse-shaped fiber amplifiers with 42 fs compressed pulse duration," Opt. Express **31**, 12717 (2023).
16. H. Chang, Q. Chang, J. Xi, *et al.*, "First experimental demonstration of coherent beam combining of more than 100 beams," Photonics Res. **8**, 1943 (2020).
17. C. Gaida, M. Gebhardt, T. Heuermann, *et al.*, "Watt-scale super-octave mid-infrared intrapulse difference frequency generation," Light Sci. Appl. **7**, 94 (2018).
18. J. Wang, R. Chen, and G. Chang, "On the frequency spanning of SPM-enabled spectral broadening: analytical solutions," Opt. Express **30**, 33664 (2022).
19. P. Zhou, L. Huang, J. Xu, *et al.*, "High power linearly polarized fiber laser: generation, manipulation and application," Sci. China Technol. Sci. **60**, 1784 (2017).
20. W. S. Brocklesby, "Progress in high average power ultrafast lasers," Eur. Phys. J. Spec. Top. **224**, 2529 (2015).
21. R. Stolen, "Polarization effects in fiber Raman and Brillouin lasers," IEEE J. Quantum Electron. **15**, 1157 (1979).
22. M. O. V. Deventer and A. J. Boot, "Polarization properties of stimulated Brillouin scattering in single-mode fibers," J. Lightwave Technol. **12**, 585 (1994).
23. G. P. Agrawal, *Nonlinear Fiber Optics, 5th* ed. (Academic Press, 2012).
24. K. Brar, M. Savage-Leuchs, J. Henrie, *et al.*, "Threshold power and fiber degradation induced modal instabilities in high-power fiber amplifiers based on large mode area fibers," Proc. SPIE **8961**, 89611R (2014).
25. R. Tao, X. Wang, and P. Zhou, "Comprehensive theoretical study of mode instability in high-power fiber lasers by employing a universal model and its implications," IEEE J. Sel. Top. Quantum Electron. **24**, 0903319 (2018).
26. C. Jauregui, C. Stihler, S. Kholaif, *et al.*, "Mitigation of transverse mode instability in polarization maintaining, high-power fiber amplifiers," Proc. SPIE **11665**, 116650V (2021).
27. G. Palma-Vega, D. Hässner, S. Kuhn, *et al.*, "TMI and polarization static energy transfer in Yb-doped low-NA PM fibers," Opt. Express **31**, 24730 (2023).
28. S. Ren, G. Wang, W. Li, *et al.*, "3 kW power-level all-fiberized superfluorescent fiber source with linear polarization and near-diffraction-limited beam quality," Appl. Opt. **61**, 3952 (2022).
29. S. Ren, P. Ma, Y. Chen, *et al.*, "5 kW-level narrow linewidth fiber laser output realized by homemade polarization-maintained fiber," Infrared Laser Eng. **52**, 20220900 (2023).
30. Y. Wang, W. Peng, H. Liu, *et al.*, "Linearly polarized fiber amplifier with narrow linewidth of 5 kW exhibiting a record output power and near-diffraction-limited beam quality," Opt. Lett. **48**, 2909 (2023).
31. G. Wang, J. Song, Y. Chen, *et al.*, "Six kilowatt record all-fiberized and narrow-linewidth fiber amplifier with near-diffraction-limited beam quality," High Power Laser Sci. Eng. **10**, e22 (2022).
32. P. Ma, T. Yao, Y. Chen, *et al.*, "New progress of high-power narrow-linewidth fiber lasers," Proc. SPIE **12310**, 123100E (2022).
33. Z. Huang, C. Liu, J. Li, *et al.*, "Fiber polarization control based on a fast locating algorithm," Appl. Opt. **52**, 6663 (2013).
34. B. Koch, A. Hidayat, H. Zhang, *et al.*, "Optical endless polarization stabilization at 9 krad/s with FPGA-based controller," IEEE Photon. Technol. Lett. **20**, 961 (2008).
35. E. Assémat, D. Dargent, A. Picozzi, *et al.*, "Polarization control in spun and telecommunication optical fibers," Opt. Lett. **36**, 4038 (2011).
36. D.-B. Wang and J.-F. Zhou, "Research on polarization control in the long distance fiber-optic sensing," Proc. SPIE **8914**, 89141B (2013).
37. G. D. Goodno, S. J. McNaught, J. E. Rothenberg, *et al.*, "Active phase and polarization locking of a 1.4 kW fiber amplifier," Opt. Lett. **35**, 1542 (2010).
38. G. D. Goodno, S. J. McNaught, M. E. Weber, *et al.*, "Multichannel polarization stabilization for coherently combined fiber laser arrays," Opt. Lett. **37**, 4272 (2012).
39. Y. Wang, Y. Feng, X. Wang, *et al.*, "6.5 GHz linearly polarized kilowatt fiber amplifier based on active polarization control," Appl. Opt. **56**, 2760 (2017).
40. R. Su, Y. Liu, B. Yang, *et al.*, "Active polarization control of a 1.43 kW narrow linewidth fiber amplifier based on SPGD algorithm," J. Opt. **19**, 045802 (2017).
41. N. Platonov, R. Yagodkin, J. De La Cruz, *et al.*, "Up to 2.5-kW on non-PM fiber and 2.0-kW linear polarized on PM fiber narrow linewidth CW diffraction-limited fiber amplifiers in all-fiber format," Proc. SPIE **10512**, 105120E (2018).
42. S. Ren, H. Chang, P. Ma, *et al.*, "3.38 kW all-fiberized narrow linewidth fiber laser based on active polarization control using RMS-Prop algorithm," Opt. Laser Technol. **166**, 109634 (2023).
43. M. Jiang, H. Wu, Y. An, *et al.*, "Fiber laser development enabled by machine learning: review and prospect," PhotoniX **3**, 16 (2022).
44. H. G. Winful, "Self-induced polarization changes in birefringent optical fibers," Appl. Phys. Lett. **47**, 213 (1985).
45. M.-J. Wang, W.-G. Jia, S.-Y. Zhang, *et al.*, "Influence of Raman effect on the state of polarization evolution in a low-birefringence fiber," Acta Phys. Sin. **63**, 104204 (2014).
46. T. Wang, C. Li, B. Ren, *et al.*, "Time jitter and intensity noise of an all-fiber high-power harmonic Mamyshev oscillator," J. Lightwave Technol. **41**, 6369 (2023).
47. B. Ren, C. Li, T. Wang, *et al.*, "All-polarization-maintaining figure-9 mode-locked Tm-doped fiber laser with amplitude noise and timing jitter suppression," J. Lightwave Technol. **41**, 733 (2023).
48. J. Kim and Y. Song, "Ultralow-noise mode-locked fiber lasers and frequency combs: principles, status, and applications," Adv. Opt. Photonics **8**, 465 (2016).